4 Wetting of Solids

Martin E. R. Shanahan[1] · *Wulff Possart*[2]
[1]Université de Bordeaux, Talence, France
[2]Saarland University, Saarbrücken, Germany

Lucas F. M. da Silva, Andreas Öchsner, Robert D. Adams (eds.), *Handbook of Adhesion Technology*,
DOI 10.1007/978-3-642-01169-6_4,

Abstract: The contact between a solid and a liquid involves the phenomenon of wetting. This is the intuitive, intimate contact between the two phases. We consider here thermodynamic aspects of wetting, which involves three phases in fact, since the environment must be taken into account. Methods for determining wetting characteristics are discussed.

4.1 What is Wetting?

When you "wet" your hands under the tap, or in a bowl of water, you are implicitly assuming that the water is directly, intimately, contacting your skin. Water is wet, apparently even etymologically. The Indo-European root of water is *wed-, "wet." However, this important, implicit connotation of the term wetting clearly fails if you are so unlucky as to break an old mercury thermometer or barometer and get the liquid on your skin. The mercury tucks itself up into little beads and apparently does not "wet" your skin. What is the fundamental difference? This can be explained by the concept of "contact angle", θ. For present purposes, it will suffice to discuss the "static" contact angle, θ_0. Let us consider the case of a small drop of liquid deposited on a flat, solid surface (Real solid surfaces are, of course, rough. The consequences will be considered below in Sect. 4.5), from an intuitive viewpoint. A *meniscus* (Greek: mēnískos = crescent), corresponding to the liquid/air environment, is formed. After *spreading* (cf. Chap. 5) to rest has occurred, a *sessile* ("sitting"), static drop of the liquid is present. Angle θ_0 is that subtended between the solid/liquid interface, and the tangent to the liquid/air interface, as shown schematically in *Fig. 4.1*. It is measured perpendicularly both to the solid surface and to the triple line of contact where solid, liquid, and air meet. (For definiteness, the surrounding medium is regarded as "air." More precisely, the surrounding gas, air or otherwise, *always* contains vapor of the liquid, and, in principle, of the solid. However, the vapor pressure of most solids is very low.)

Of course, the gas phase could be a second liquid, provided it has a miscibility gap with the first liquid. Henceforth, the environing phase will generally be referred to as "vapor," while bearing in mind the previous comment. Referring to *Fig. 4.1*, it may be seen that the case on the left represents a contact angle of less than 90° ($\pi/2$ rad), and may be called "good wetting," whereas that on the right is such that $\theta_0 > 90°$, and this represents "poor wetting." In the extreme case of $\theta_0 \to 0$, the liquid becomes a thin film (for example, oil deposited on a steel sheet). This is often called *spreading*. Although it will not be treated here, the thickness of such films depends on long-range molecular forces, which may span the entire liquid thickness of the film, leading to what is effectively "interference" between the two interfaces, liquid–solid and vapor–liquid (cf. Chap. 5). However, this is beyond the scope of the present chapter as such spreading is fundamentally different from simple wetting. At the other extreme, the case of $\theta_0 \to 180°$: non-wetting, may be considered. This cannot, in fact, exist if the solid is truly smooth and if the environment is only gaseous but can in some cases when two liquids are involved (Shanahan et al. 1982).

The importance of contact angle is that it determines the extent of (solid) surface coverage by a liquid. It is intuitively clear that the interfacial area covered by a sessile drop of given, fixed volume V of liquid increases as contact angle decreases, but this may be readily written formally in the case of a spherical, cap-shaped drop, of contact radius r, and height h. Writing $t = \tan(\theta_0/2) = h/r$, and with a standard trigonometric formula for the volume, V, of

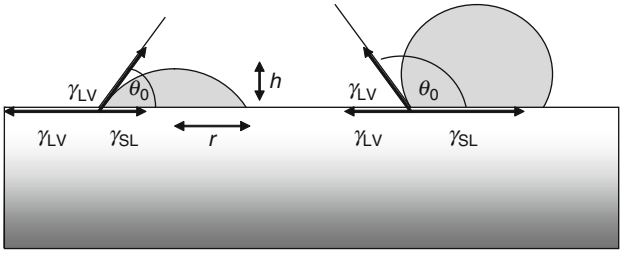

Fig. 4.1

Schematic representation of low (*left*) and high (*right*) static contact angles, θ_0. Interfacial tensions are represented by *arrows* and termed γ_{IJ} (S = solid, L = liquid, V = vapor/surrounding fluid phase)

a spherical segment: $V = \pi\ h\ (3r^2 + h^2)/6$, it is readily shown that the contact area, A, is given by:

$$A = \pi \cdot r^2 = \pi^{1/3}\left[\frac{6\,V}{t\,(3 + t^2)}\right]^{2/3} \tag{4.1}$$

In the range of possible contact angles, $0^\circ \leq \theta_0 \leq 180^\circ$, t is a monotonically increasing function of θ_0, and therefore, A increases as θ_0 decreases, at constant V.

So, decreasing θ_0 implies better coverage, or wetting, but what controls θ_0? Between the solid and liquid, and liquid and vapor phases, there are *phase boundaries* of the different substances. These can be imagined as 2D faces, or interfaces, but nature is never so clear-cut, and a vague transition zone, the interphase, typically of the order of a few nm (nanometers) or a few tens of nm thick constitutes the changeover. It has to be mentioned that an interphase and its width is not a uniquely defined thing as it has to be attributed to the macroscopic physical or chemical quantity of interest. In other words, each thermodynamic quantity of a heterogeneous system can possess its particular spatial function across its own interphase. The interphase will be considered in Sects. 4.2 and 4.3. However, accepting as a first approximation that 2D interfaces separate phases, it can be seen in the typical case exemplified in *Fig. 4.1* that there are three *interfaces*: SL, LV, and SV (S = solid, L = liquid, V = vapor/surrounding medium), each of which has associated with it an *interfacial tension* γ_{IJ} where I and J refer to S, L, and V (see Sect. 4.2 for definition). Note that the very concept of "force/distance" is meaningless in absolute terms, since the force will have no area to "pull" or "push" on: the idea of a "stress" becomes vague. In fact, it is Gibbs' concept of "surface excess" (cf. Sect. 4.2) which allows one to see that the forces are, in fact, acting over a thin layer at the interface, and thus the concept of stress is still valid. The three phases, and therefore interfaces, meet at the drop periphery, at what is termed term the *triple line*, or *contact line*. Again, this is not really a line, but a "tube," but the concept of line is adequate in Gibbs' treatment. A force balance between the various γ_{IJ} exists at the triple line and, at equilibrium, this is principally what governs the value of θ_0 (see below for details).

Accepting the concept of contact angle, its importance may be appreciated in many sectors, biological and industrial. Without resort to equations, it is intuitive (and correct) to realize that it is more difficult to remove an oil film from steel (contact angle ca. 0°) than a drop of mercury from glass (contact angle ca. 130°). Not only is adherence of the oil intrinsically better, but for a given

volume, coverage is superior. The same, of course, has to apply to paints and inks. If an insecticide is applied to a leaf, it is clearly inefficient if, when the leaf slopes, the liquid simply rolls off. Therefore, a small, preferably zero, contact angle is required. In the case of adhesives, this significant coverage and propensity to wet the solid in contact is crucial in forming a good bond as it gives the molecules the *opportunity* to form adhesive interactions, even if the "true," chemical, bond is produced later by hardening of the adhesive (drying, chemical reaction, cooling). If the surface is rough, the same wetting tendency will help ensure filling the interstices. This not only increases true contact area, but reduces stress concentrations, liable to be crack initiators.

There are, of course, many cases where *poor* wetting is required. Nature masters this beautifully in the case of, for example, duck feathers and lotus leaves (Zhang et al. 2009). Mankind attempts to exploit it with PTFE and other polymers as cooking utensil coatings and raincoat treatments.

The main objective of this chapter is to consider in more detail the phenomenology of wetting, specifically in the static case (kinematics are covered in ❯ Chap. 5). In other words, the triple phase line will principally be considered to be at rest. The description will now be couched in terms of the needs of thermodynamic equilibrium.

4.2 Thermodynamics of a Phase Boundary: An Introduction

As mentioned above, the boundary between two thermodynamic phases has to be a vague transition zone for any physical quantity because nature does not like sharp steps. Hence, in principle, any real phase boundary extends in three dimensions – the *interphase* (cf. ❯ *Fig. 4.2a*). This apparently innocent comment has the important result that all extensive thermodynamic quantities, such as concentrations, energies, entropy etc., will depend on position across the interphase. This causes trouble when it comes to an exact description of a thermodynamic system with more than one phase, because there is virtually no experimental access to the spatial dependence of thermodynamic quantities across the phase boundary. Moreover, the beauty of usual thermodynamics is very much due to the assumption that parameters remain constant across a phase.

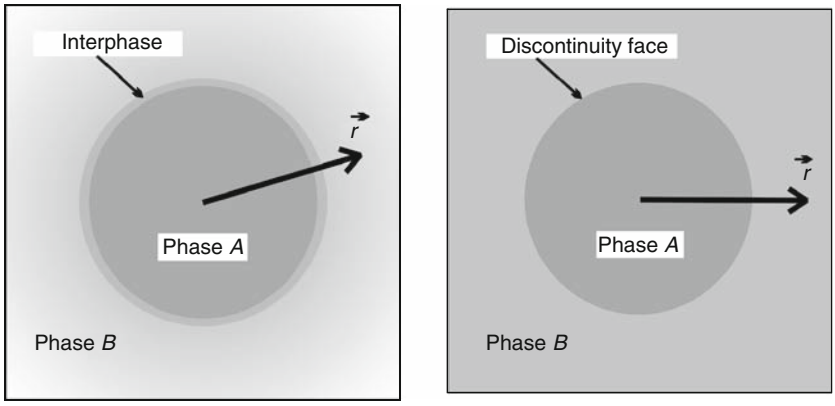

Fig. 4.2

Schematic drawing for an interphase in a radially configuration of spherical symmetry of two phases *A* and *B*. The interphase shown in (a) (*left*) is replaced by the 2D discontinuity face (b) (*right*) in interface thermodynamics

The exact volume V of such a two-phase system is given by the total

$$V = V_A + V_B + V_{\text{Interphase}} \tag{4.2}$$

where the terms on the right hand side refer, respectively, to the two "bulk" phases and to the interphase. Hence, a method to circumvent the problem is needed. A pioneer in this subject (among many others!) was J.W. Gibbs, who introduced in a standardized way the notion of a "discontinuity" (Bumstead and Van Name 1961, Gaydos et al. 1996). A brief version of this thermodynamic description for phase boundaries is now introduced.

4.2.1 Brief Description of Gibbs' Model for a Phase Boundary

The "real" interphase (Bakker 1902) is replaced by the "artificial" *discontinuity face* (D-face) with a certain area A^{D}_{AB} – cf. *Fig. 4.2b*. (For example, see (Rusanov 1978, Rusanov and Prokhorov 1996) for more details.) The position of the D-face can be chosen *arbitrarily, but only once,* from the theoretical point of view or, in measurements, is fixed by the experiment itself. Indeed, the experimenter is not able to select the position of the D-face deliberately. Usually, he even does not know that position exactly. Although the D-face and the interface are very similar in many cases, the term "D-face" will be used here because similarity does not mean identity from the theoretical viewpoint. As a first consequence, (4.2) has to be replaced by

$$V = V_A + V_B \tag{4.3}$$

for the two-phase system, i.e., the interphase volume $V_{\text{Interphase}}$ is "eliminated," being arbitrarily attributed partially to each of phases A and B according to the position given of the D-face.

Moreover, the balance of any extensive thermodynamic quantity, Y, in the two-phase system is no longer

$$Y = Y_A + Y_B + Y_{\text{Interphase}} \tag{4.4}$$

but is written as

$$Y = Y_A + Y_B + Y^{\mathrm{D}}_{AB} \tag{4.5}$$

Here, Y^{D}_{AB} denotes the *excess of* Y with respect to the D-face. It is a correction that guarantees the correct value for Y in the whole two-phase system after the interphase has been ignored. Note that any excess quantity can adopt positive and negative values as well. Now, the extensive Y can be referred to the D-face area A^{D}_{AB}, thus providing the corresponding intensive quantity y

$$y = \frac{Y}{A^{\mathrm{D}}_{AB}} = y_A + y_B + y^{\mathrm{D}}_{AB} \tag{4.6}$$

For example, the number of moles n_i of a component i in the system

$$n_i = n_{i,A} + n_{i,B} + n_{\text{Interphase}} \tag{4.7a}$$

$n_{i,A}$, $n_{i,B}$, $n_{Interphase}$ = number of moles of component i in phases A, B and in the interphase is replaced by

$$n_i = n_{i,A} + n_{i,B} + n^{\mathrm{D}}_{\mathrm{i},AB} = c_{i,A} \cdot V_A + c_{i,B} \cdot V_A + n^{\mathrm{D}}_{\mathrm{i},AB} \tag{4.7b}$$

$n^{\mathrm{D}}_{\mathrm{i},AB}$ = excess number of moles of i for the given D-face
$c_{i,A}$, $c_{i,B}$ = concentrations of i (mole m^{-3}) in phases A, B

A simple rearrangement of (4.7b) provides the definition of the *absolute adsorption of component i* in a thermodynamic system with N components

$$\Gamma^{\mathrm{D}}_{i,AB} \overset{def}{=} \frac{n^{\mathrm{D}}_{i,AB}}{A^{\mathrm{D}}_{AB}} = \frac{n_i - c_{i,A} \cdot V_A - c_{i,B} \cdot V_A}{A^{\mathrm{D}}_{AB}} \quad \text{with} \quad i = 1 \ldots N \tag{4.8}$$

Indirectly, these N excess quantities replace the concentration profiles of all components in the system. Obviously, the value for any of the $\Gamma^{\mathrm{D}}_{i,AB}$ depends on A^{D}_{AB} and hence on the position for the D-face. As that position can be chosen only once for a given phase boundary, only one of the $\Gamma^{\mathrm{D}}_{i,AB}$ can be made zero while all other $(N-1)$ $\Gamma^{\mathrm{D}}_{j,AB}$ adopt nonzero values (This naïve statement will be important for the coming discussions).

The *interfacial tension* is another very important quantity for the thermodynamics of interfaces. The starting point stems from continuum mechanics for deformable solids where the balance of forces at point $\vec{r}$ in the solid is given by

$$\frac{d\vec{F}(\vec{r})}{dV} = \vec{f}(\vec{r}) = Div\ \vec{\sigma}(\vec{r}) \tag{4.9}$$

$\vec{f}(\vec{r})$ = density of the external force that deforms a solid
$\vec{\sigma}(\vec{r})$ = tensor of internal stresses in the deformed solid
and the mechanical work of deformation ΔW of the volume V

$$\Delta W = \int_V \sum_{i,k} (\sigma_{ik} \cdot \delta e_{ik})\ dV \tag{4.10}$$

σ_{ik}, δe_{ik} = components of the stress and the deformation tensors, $\vec{\sigma}(\vec{r})$, $\vec{e}(\vec{r})$, respectively.

In thermodynamics, pressure is preferred, but now it is a tensor which is defined as

$$\vec{p}(\vec{r}) = -\vec{\sigma}(\vec{r}) \tag{4.11}$$

All three tensors $\vec{\sigma}(\vec{r})$, $\vec{p}(\vec{r})$, $\vec{e}(\vec{r})$ are symmetric and hence they can be transformed into diagonal form, provided a suitable system of coordinates is chosen. Then, the analysis of (4.10) for the boundary between the two phases will provide a definition for interfacial tension. As an illustration, the derivation is considered for the case of an *isotropic horizontal planar phase boundary*. The D-face spans the *x,y*-plane of the Cartesian coordinate system and the *z*-axis is parallel to, but in the opposite direction to, the gravitational force which is the external field here

$$\vec{f}(z) = -g \cdot \rho(z) \cdot \vec{k} \tag{4.12}$$

g = gravity acceleration, $\rho(z)$ = mass density, $\vec{k}$ = unit vector for z-direction.

From (Eqs. 4.9, 4.11, 4.12), it follows that

$$Div \begin{pmatrix} p_{xx} & 0 & 0 \\ 0 & p_{yy} & 0 \\ 0 & 0 & p_{zz} \end{pmatrix} = \begin{pmatrix} \frac{\partial p_{xx}}{\partial x} \\ \frac{\partial p_{yy}}{\partial y} \\ \frac{\partial p_{zz}}{\partial z} \end{pmatrix} = \begin{pmatrix} 0 \\ 0 \\ -g \cdot \rho(z) \end{pmatrix}$$

and hence

$$p_{xx}(z) = const; \quad p_{yy}(z) = const; \quad p_{zz}(z) - p = -g \cdot \int_{-\infty}^{z} \rho(z)\, dz \qquad (4.13a - c)$$

p = isostatic external pressure.

The two tangential pressure components p_{xx} and p_{yy} have to be equal for any z, by symmetry

$$p_{xx}(z) = p_{yy}(z) \equiv p_T(z) \qquad (4.13d)$$

p_T = pressure in the x,y-plane at z

Usually, the interphase is very thin ($d \approx 10^{-9}$–10^{-7} m) and (4.13c) can be approximated by

$$g \cdot \int_{-\frac{d}{2}}^{\frac{d}{2}} \rho(z)\, dz \approx 0 \quad \rightarrow \quad p_{zz}(z) \equiv p_N \approx p = const \qquad (4.13e)$$

p_N = pressure component in z-direction.

With (4.13), (4.10) is now

$$\begin{aligned}
\Delta W &= -\int_V \left[p_T \cdot \left(\delta e_{xx} + \delta e_{yy}\right) + p \cdot \delta e_{zz}\right] dV \\
&= -\int_V \left[p_T \cdot \left(\delta e_{xx} + \delta e_{yy}\right) - p \cdot \left(\delta e_{xx} + \delta e_{yy}\right) + p \cdot \left(\delta e_{xx} + \delta e_{yy}\right) + p \cdot \delta e_{zz}\right] dV \\
&= \int_V \left[(p - p_T) \cdot \left(\delta e_{xx} + \delta e_{yy}\right)\right] dV - p \cdot \int_V \left(\delta e_{xx} + \delta e_{yy} + \delta e_{zz}\right) dV
\end{aligned}$$

and for small deformations

$$\Delta W = \Delta A_{AB}^{D} \cdot \int_{-\infty}^{\infty} (p - p_T)\, dz - p \cdot \Delta V \qquad (4.14a)$$

The second term is the well-known work of volume expansion while the first term

$$\Delta W_{AB}^{D} = \Delta A_{AB}^{D} \cdot \int_{-\infty}^{\infty} (p - p_T)\, dz \qquad (4.14b)$$

gives the work for increasing the area of the D-face by ΔA_{AB}^{D}.

Equation (4.14) implies the definition of the *interfacial tension for the* chosen isotropic planar D-face:

$$\gamma_{AB}^{D} \overset{def}{=} \int_{-\infty}^{\infty} (p - p_T)\, dz \qquad (4.15a)$$

With an assumed *spherical shape for the isotropic interphase*, a similar mathematical treatment provides the *interfacial tension for the spherical D-face of radius* r_D

$$\gamma_{AB}^{\mathrm{D}} = \frac{1}{r_D^2}\left[\int_0^{r_D}(p_A - p_T)\, r^2\, dr + \int_{r_D}^{\infty}(p_B - p_T)\, r^2\, dr\right] \tag{4.15b}$$

p_A, p_B = isostatic pressures inside the phases A, B. They are different due to the curved interphase.

These two examples illustrate that γ_{AB}^{D} is, in general, an excess quantity for a given D-face. As a consequence of this result, there is no physical difference between interfacial and surface tension in thermodynamic equilibrium. In the literature, the term surface tension is attributed to the D-face, or interface, between a condensed phase and the corresponding vapor phase. Some authors define the surface tension as the interfacial tension of a condensed phase in contact with vacuum. This is incorrect in the framework of equilibrium thermodynamics. A condensed phase will fill a vacuum with its vapor phase to be at thermodynamic equilibrium. Hence, any interfacial tension results from a defined pair of phases, never from a single phase, and they need to be marked by the subscript "*AB*" or similar. Otherwise, the interfacial tension would be ill-defined. γ_{AB}^{D} accounts for the real distribution of pressure or stress inside the phase boundary. It is called a tension because it possesses the dimension of a force per unit length [$\mathrm{N\,m^{-1}}$] in the 2D space of the D-face, and indeed acts somewhat like a tension in a membrane (except there is no elastic proportionality between the tension and extension). Moreover, (4.15b) reveals that the value for γ_{AB}^{D} usually depends on the position, here r_D, chosen for that D-face. γ_{AB}^{D} is always positive. This is a condition of stability for the interphase and hence for the phase itself, and it is proven by experiment and by statistical mechanics calculations as well. The value remains almost constant when p decreases. Therefore, p_T must be negative, at least inside the dominant part of the interphase, and as a consequence, the interphase and the corresponding D-face will adopt the minimum volume and area, respectively.

To apply thermodynamic energy balances (1st law), knowledge of how *mechanical work* changes the state of the system must be available. As the phase boundary is included, the usual equations have to be revised. *Fig. 4.3* depicts the situation for the volume expansion δV of the phase A that is accompanied by a change of the principal radii of curvature from R_1, R_2 to $(R_1 + \delta z)$, $(R_1 + \delta z)$, respectively.

Now, the mechanical work can be split into *four parts*. The first one comes from the work of volume expansion

$$\delta W^{\mathrm{V}} = -p_A \cdot dV_A - p_B \cdot dV_B \tag{4.16a}$$

Part two results from the corresponding increase of area of the D-face according to (4.14b)

$$\delta W_{AB}^{\mathrm{D}} = \gamma_{AB}^{\mathrm{D}} \cdot dA_{AB}^{\mathrm{D}} \tag{4.16b}$$

The increase of D-face area can be accompanied by a change of the radii of curvature. This corresponds to the third contribution to the mechanical work:

$$\delta W_{\mathrm{curvature}}^{\mathrm{D}} = A_{AB}^{\mathrm{D}} \cdot C_1 \cdot d\left(\frac{1}{R_1}\right) + A_{AB}^{\mathrm{D}} \cdot C_2 \cdot d\left(\frac{1}{R_2}\right) \tag{4.16c}$$

C_1, C_2 = proportionality factors.

The fourth and last part is related to the action of external forces such as gravity. The D-face possesses the total excess mass

$$m_{AB}^{\mathrm{D}} = \sum_{i=1}^{N} m_{i,AB}^{\mathrm{D}} = \sum_{i=1}^{N} M_i \cdot n_{i,AB}^{\mathrm{D}} = A_{AB}^{\mathrm{D}} \cdot \sum_{i=1}^{N} M_i \cdot \Gamma_{i,AB}^{\mathrm{D}}$$

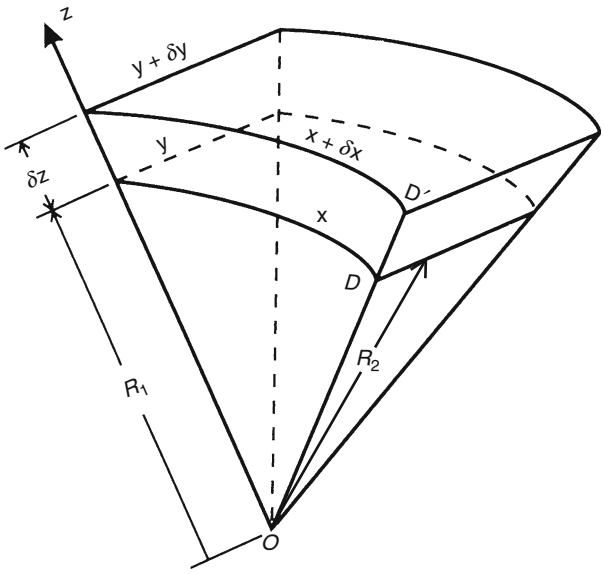

Fig. 4.3
Geometric scheme for the of the volume increase δV of a phase A with a curved D-face (D→D')

which is raised by a height dh when the D-face shifts in the gravitational field. Hence, the corresponding work is

$$\delta W^{\mathrm{D}}_{\mathrm{gravitation}} = A^{\mathrm{D}}_{AB} \cdot \sum_{i=1}^{N} \left(M_i \cdot \Gamma^{\mathrm{D}}_{i,AB} \right) \cdot g \cdot dh \tag{4.16d}$$

In total, the work sums up to

$$\begin{aligned} \delta W = & - p_A \cdot dV_A - p_B \cdot dV_B + \\ & + \gamma^{\mathrm{D}}_{AB} \cdot dA^{\mathrm{D}}_{AB} + A^{\mathrm{D}}_{AB} \cdot C_1 \cdot d\left(\frac{1}{R_1}\right) + A^{\mathrm{D}}_{AB} \cdot C_2 \cdot d\left(\frac{1}{R_2}\right) + \\ & + A^{\mathrm{D}}_{AB} \cdot \sum_{i=1}^{N} \left(M_i \cdot \Gamma^{\mathrm{D}}_{i,AB} \right) \cdot g \cdot dh \end{aligned} \tag{4.16f}$$

In this equation, however, the work would seem to depend on A^{D}_{AB} and hence on the arbitrarily chosen position of the D-face. This is impossible from a physical point of view and terms of (4.16f) must clearly correct for this implicitly. The paradox is revealed from a virtual displacement δN of the D-face along its normal $\vec{N}$. The corresponding virtual mechanical work is $\delta W = 0$. Another expression available is

$$\delta V_A = A^{\mathrm{D}}_{AB} \cdot \delta N, \quad \delta V_B = -A^{\mathrm{D}}_{AB} \cdot \delta N, \quad dA^{\mathrm{D}}_{AB} = A^{\mathrm{D}}_{AB} \left(\frac{1}{R_1} + \frac{1}{R_1} \right) \delta N, \quad \delta N = \delta R_1 = \delta R_2$$

and (4.16f) now provides the *generalized Laplace equation*

$$p_A - p_B = \gamma^{\mathrm{D}}_{AB}\left(\frac{1}{R_1}+\frac{1}{R_2}\right) - \frac{C_1}{R_1^2} - \frac{C_2}{R_2^2} + \sum_{i=1}^{N}\left(M_i \cdot \Gamma^{\mathrm{D}}_{i,AB}\right)\cdot g \cdot \cos\varphi \tag{4.17a}$$

where φ = angle between $\vec{N}$ and vertical direction.

The complete condition for mechanical equilibrium of a two-phase system with a curved phase boundary in a gravitational field is now available. It shows that the pressure difference between two curved phases depends on the properties of the D-face: interfacial tension, curvature, and adsorptions $\Gamma^{\mathrm{D}}_{i,AB}$.

Usually, the absolute adsorptions $\Gamma^{\mathrm{D}}_{i,AB}$, as well as C_1 and C_2, are small. Then, the following approximation of (4.17a) can be used:

$$p_A - p_B = \gamma^{\mathrm{D}}_{AB}\left(\frac{1}{R_1}+\frac{1}{R_2}\right) \tag{4.17b}$$

This is known as Laplace's equation.

For an *anisotropic* phase boundary like in the case of oriented molecules, the interfacial tension becomes a diagonal tensor

$$\vec{\gamma}^{\mathrm{D}}_{AB} = \begin{pmatrix} \gamma_{11} & 0 \\ 0 & \gamma_{22} \end{pmatrix} \tag{4.18a}$$

and the trace of the tensor provides the value for the interfacial tension

$$\gamma = \frac{1}{2}(\gamma_{11} + \gamma_{22}) \tag{4.18b}$$

Finally, the corresponding forms of Equations (4.17) are

$$p_A - p_B = \frac{\gamma^{\mathrm{D}}_{11}}{R_1} + \frac{\gamma^{\mathrm{D}}_{22}}{R_2} - \frac{C_1}{R_1^2} - \frac{C_2}{R_2^2} + \sum_{i=1}^{N}\left(M_i \cdot \Gamma^{\mathrm{D}}_{i,AB}\right)\cdot g \cdot \cos\varphi \tag{4.19a}$$

$$p_A - p_B = \frac{\gamma^{\mathrm{D}}_{11}}{R_1} + \frac{\gamma^{\mathrm{D}}_{22}}{R_2} \tag{4.19b}$$

With these results, the energy balance of the two-phase system can now be evaluated in detail.

4.2.2 Energy Balance for a Two-Phase System: Thermodynamic Potentials

The *thermodynamic potential for the internal energy U* in any thermodynamic system provides the starting point

$$dU = T \cdot dS + \delta W + \sum_i \mu_i \cdot dm_i$$

T = absolute temperature, S = entropy μ_i, m_i = chemical potential and mass of component i.

Using (4.5, 4.16f) for a system with the isotropic phases A and B, the following relation is obtained

$$\begin{aligned} dU &= dU_A + dU_B + dU_{AB}^{\mathrm{D}} \\ &= T \cdot \left(dS_A + dS_B + dS_{AB}^{\mathrm{D}}\right) - p_A \cdot dV_A - p_B \cdot dV_B + \\ &+ \gamma_{AB}^{\mathrm{D}} \cdot dA_{AB}^{\mathrm{D}} + A_{AB}^{\mathrm{D}} \cdot C_1 \cdot d\left(\frac{1}{R_1}\right) + A_{AB}^{\mathrm{D}} \cdot C_2 \cdot d\left(\frac{1}{R_2}\right) + \\ &+ A_{AB}^{\mathrm{D}} \cdot \sum_{i=1}^{N} \left(M_i \cdot \Gamma_{i,AB}^{\mathrm{D}}\right) \cdot g \cdot dh + \sum_i \mu_i \cdot \left(dm_{i,A} + dm_{i,B} + dm_{i,AB}^{\mathrm{D}}\right) \end{aligned} \tag{4.20}$$

The terms for the D-face are easily identified. For clarity and brevity, however, the following treatment is restricted to *a plane interface* and *neglect gravity*. Then, (4.20) reduces to

$$\begin{aligned} dU = dU_A + dU_B + dU_{AB}^{\mathrm{D}} = T \cdot \left(dS_A + dS_B + dS_{AB}^{\mathrm{D}}\right) - p_A \cdot dV_A - p_B \cdot dV_B + \\ + \gamma_{AB}^{\mathrm{D}} \cdot dA_{AB}^{\mathrm{D}} + \sum_i \mu_i \cdot \left(dm_{i,A} + dm_{i,B} + dm_{i,AB}^{\mathrm{D}}\right) \end{aligned} \tag{4.21}$$

Integration provides the full internal energy of the two-phase system

$$\begin{aligned} U = T\left(S_A + S_B + S_{AB}^{\mathrm{D}}\right) - p_A V_A - p_B V_B + \\ + \gamma_{AB}^{\mathrm{D}} A_{AB}^{\mathrm{D}} + \sum_i \mu_i \cdot \left(m_{i,A} + m_{i,B} + m_{i,AB}^{\mathrm{D}}\right) \end{aligned} \tag{4.22}$$

and the *excess internal energy of the force-free plane D-face*

$$U_{AB}^{\mathrm{D}} = T \cdot S_{AB}^{\mathrm{D}} + \gamma_{AB}^{\mathrm{D}} A_{AB}^{\mathrm{D}} + \sum_i \mu_i \cdot m_{i,AB}^{\mathrm{D}} \tag{4.23}$$

Now, *specific* quantities are introduced

$$u_{AB}^{\mathrm{D}} = \frac{U_{AB}^{\mathrm{D}}}{A_{AB}^{\mathrm{D}}} = T \cdot s_{AB}^{\mathrm{D}} + \gamma_{AB}^{\mathrm{D}} + \sum_i \mu_i \cdot \Gamma_{i,AB}^{\mathrm{D}} \tag{4.24}$$

$$s_{AB}^{\mathrm{D}} = \frac{S_{AB}^{\mathrm{D}}}{A_{AB}^{\mathrm{D}}} = \text{specific excess entropy of the D} - \text{face.}$$

in order to get intensive thermodynamic quantities.

Moreover, the *excess Helmholtz free energy* is

$$F_{AB}^{\mathrm{D}} = U_{AB}^{\mathrm{D}} - T \cdot S_{AB}^{\mathrm{D}} = \gamma_{AB}^{\mathrm{D}} A_{AB}^{\mathrm{D}} + \sum_i \mu_i \cdot m_{i,AB}^{\mathrm{D}} \tag{4.25}$$

with the corresponding *specific excess Helmholtz free energy*

$$f_{AB}^{\mathrm{D}} = \frac{F_{AB}^{\mathrm{D}}}{A_{AB}^{\mathrm{D}}} = u_{AB}^{\mathrm{D}} - T \cdot s_{AB}^{\mathrm{D}} = \gamma_{AB}^{\mathrm{D}} + \sum_i \mu_i \cdot \Gamma_{i,AB}^{\mathrm{D}} \tag{4.26}$$

These results give access to the *interfacial tension as a thermodynamic excess quantity of the force-free plane D-face*. Note that the interfacial tension *and* the absolute adsorptions of all components contribute to the interfacial energy, both the specific excess internal energy and the specific excess Helmholtz free energy. At a first glance, this statement is very natural, indeed. In the literature, however, interfacial tension and interfacial energy are very often considered as synonyms. Clearly, this is wrong.

Finally, the total differential for (4.23) is derived and compared with the corresponding terms in (4.21). This yields the *Gibbs adsorption equation*

$$d\gamma_{AB}^{D} = -s_{AB}^{D}\, dT - \sum_i \Gamma_{i,AB}^{D}\, d\mu_i \tag{4.27}$$

Equation (4.27) depicts the interfacial tension as a function of temperature, and, via the chemical potentials, of pressure and composition of the two-phase system.

4.3 Thermodynamic Equilibrium of Three Phases: Basics

From Sect. 4.1, it is clear that wetting and the contact angle depend on all *three* contacting phases. Hence, the Gibbs concept of excess quantities as thermodynamic quantities for phase boundaries has to be extended in an appropriate way. For a sessile drop on a *flat*, *homogeneous* solid, the situation is illustrated in *Fig. 4.4*. The three phases create a new microscopic boundary region at their "line" of common contact. For the sessile drop, this region forms a curved tube along the rim of the drop on the solid. Inside the tube, the three D-faces for the three two-phase boundaries respond by deforming, shown very much exaggerated in the drawing.

The real three-phase region (tube) is replaced by a *triple line* (TL) as the new model element for thermodynamic considerations. In theory, its position results from the extrapolation of the three *undisturbed* D-faces to their common intersection. Accordingly, the tangent lines on these extrapolated D-faces D_{SL} and D_{LV} to the point of intersection lead *by definition* to the *thermodynamic contact angle* θ_e. For reasons of exactness, θ_e is introduced for the thermodynamic equilibrium of the three-phase system. The static contact angle θ_0 in Sect. 4.1 refers to the triple line at rest, i.e., to mechanical equilibrium which is a necessary but insufficient condition for thermodynamic equilibrium. θ_e is the first excess quantity for the TL. As the position of any of the three D-faces can be chosen arbitrarily, the position of the TL and the value for θ_e are arbitrary too. Fortunately, this vagueness is of no serious consequence as long as the two-phase and three-phase boundaries possess microscopic thicknesses. Note that θ_e is

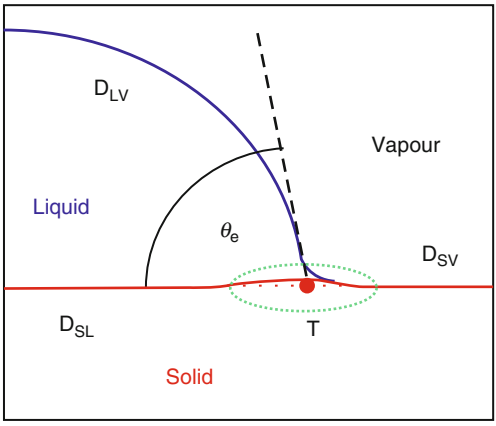

Fig. 4.4
Sketch of the cross section through a sessile drop of liquid L on a *flat* solid S, both immersed in their common vapor atmosphere V. The D-faces D_{LV}, D_{SV}, and D_{SL} describe the corresponding phase boundaries. T marks the triple line as the new model element for the three-phase boundary region (⋯) between the phases S, L, and V. θ_e = contact angle in thermodynamic equilibrium

a *local property* of the given TL in thermodynamic equilibrium. Hence, for isotropic phases, θ_e possesses one and only one value!

The pressure tensor $\vec{p}$ will also vary in the three-phase region as compared with the two-phase boundary. Hence, a *line tension* κ_{SLV} has to be introduced as the corresponding excess quantity for the TL. Although the mathematical derivation is omitted here, κ_{SLV} follows from the same physical arguments that resulted in the definition of the interfacial tension in Sect. 4.2. It acts along the tangent of any point of the TL and has the dimension of a force as it refers to a tension in a 1D space.

By analogy with a D-face, new excess quantities have to be introduced for all extensive thermodynamic quantities with respect to the TL. Details are not given here. For brevity, only a result of consideration of the Helmholtz free energy for a three-phase system in thermodynamic equilibrium *under the influence of gravity* is mentioned. It leads to a condition for the *mechanical equilibrium at the TL on a solid with an arbitrary surface profile* (*roughness*):

$$\gamma_{SV} = \gamma_{SL} + \gamma_{LV} \cdot \cos\theta_e + \left(\frac{\kappa_{SLV}}{R_0} + \frac{d\kappa_{SLV}}{dR_0}\right) \cdot |\cos\varphi_S| \tag{4.28}$$

γ_{IJ} = interfacial tension of the D_{IJ}-face far from the TL, R_0 = radius of curvature in the considered point of the TL, φ_S = angle of inclination of the extrapolated D_{SV}-face in the considered point of the TL.

Accordingly, θ_e does not only depend on the three interfacial tensions but also on the line tension and on the curvature of the TL. κ_{SLV} is of the order of 10^{-10} N for solids in general. Nevertheless, it deserves attention when the phases are soft and one of the contacting phases becomes very small.

Fig. 4.5 illustrates the situation for a sessile liquid drop on a *rough homogeneous* solid surface. θ_e is defined as before. However, the true value of θ_e cannot be obtained from the plane optical projection of the sessile drop anymore as the experimenter cannot look into the local surface profile in order to get the local inclination of the tangent on the D_{SL}-face.

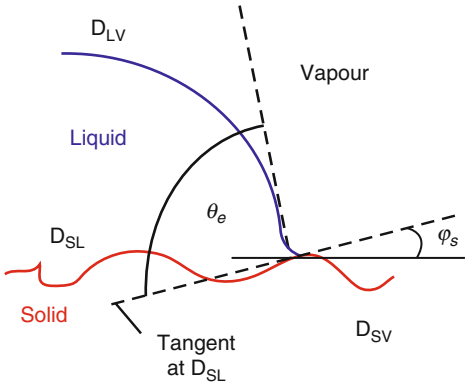

Fig. 4.5

Schematic cross section through a sessile liquid drop on a *rough* solid, both immersed in their common vapor. Now, the tangent on the extrapolated D_{SL}-face at a selected point of the TL is inclined according to the solid surface profile. θ_e is defined as before

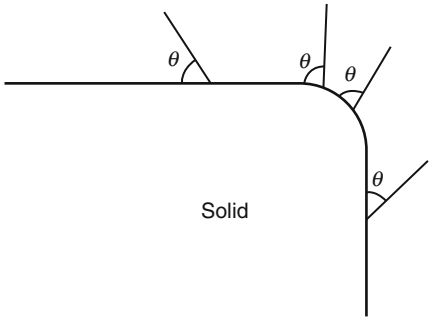

Fig. 4.6
Schematic cross section through a sharp solid edge with the constant local θ_e of a moving TL (liquid meniscus not shown)

In experiments, it seems as if the contact angle varies substantially whenever the TL moves over a sharp edge. *Fig. 4.6* shows that this is just an optical illusion because the experimenter cannot resolve the local microscopic curvature of the edge. At a *very* sharp, angle on the solid, the contact angle may be considered to become indeterminate, an effect known as *canthotaxis*. However, this proposition assumes continuum mechanics, which clearly breaks down at this scale.

4.4 Experimental Aspects of Static Wetting

In Sects. 4.2 and 4.3 the concept of interfacial tension and interfacial free energy was defined, as was noted their importance in wetting, without going into details.

For TLs with large radii of curvature ($R_0 > 10^{-6}$ m), (4.28) can be approximated by

$$\gamma_{SV} = \gamma_{SL} + \gamma_{LV} \cdot \cos\theta_e \tag{4.29}$$

The thermodynamic contact angle is still a local excess property of the TL. Treating the γ_{IJ} as tensions (i.e., with dimensions of force/distance... or mass/time^2 in some old literature!), as opposed to energies (i.e., dimensions of energy/area), in *Fig. 4.1a* balance of tensions at the triple line may be considered. This results directly in (4.29). This classic equation is referred to usually as *Young's* equation, although Thomas Young never, in fact, wrote the expression in his often-cited paper (Young 1805)! If it is preferred to treat the γ_{IJ} as interfacial free energies, and apply a simple argument of "virtual work," the same relation is obtained. Having applied a force balance horizontally, this must be possible vertically, so what "resists" $\gamma_{LV} \sin\theta_e$? Strictly, the action of tensions at the TL, specifically γ_{LV}, deforms the solid surface, but it is only under conditions in which the solid is very soft that the effect is noticeable. The slight "bump" on the solid in *Fig. 4.4* has a height given approximately by $G \cdot \gamma_{LV} \cdot \sin\theta_e$, where G represents the (elastic) shear modulus of the solid. Simple insertion of typical values shows that the effect becomes noticeable only for $G < \approx 1$ MPa (Shanahan and de Gennes 1986).

As an example, aluminum has a value of G of ca. 25 GPa, and for water γ_{LV} is ca. 70 mN m^{-1}. Taking $\sin\theta_e$ as 1, it is found that the "wetting ridge" height is ca. $3 \cdot 10^{-12}$ m: well below atomic dimensions and thus meaningless in a continuum approach! In general, the effect perpendicular to the solid is negligible. However, the wetting ridge can be significant on soft solids and even modify wetting kinetics (Shanahan and Carré 1995).

In (4.29), it may be noted that each surface tension has two suffixes representing two of the three, S, L, and V, although the use of $\gamma_{LV} = \gamma_L$ or $\gamma_{SV} = \gamma_S$ often found in the literature. In the case of the solid, γ_{SV} changes a lot when it shares a common vapor phase with a liquid because the significant part of the surrounding vapor is due to the liquid. In the above thermodynamic treatment, allowance is already made for this effect. However, many workers prefer to adopt the alternative notion of equilibrium spreading pressure, $\pi_e = \gamma_S - \gamma_{SV}$, where γ_{SV} means the solid surface tension in presence of a liquid now. π_e is often considered negligible for low activity solids, such as polymers. (*Fig. 4.15* below demonstrates that this assumption should be checked!)

The importance of (4.29) is that it may, in principle, allow one to estimate the surface tension of a solid, γ_{SV}, albeit indirectly, from knowledge of the surface tensions, γ_{LV}, of "probe" liquids, and their contact angles on the solid surface in question. Knowledge of γ_{SL} is required too, and the problem is considered in Sect. 4.5 and Chap. 6.

Whereas liquid surface tension is readily measured (see below), that of a solid is inaccessible directly from experiment due to the intrinsic lack of molecular mobility. Firstly, liquid tension will be considered.

4.4.1 Liquid Surface Tension

4.4.1.1 Maximum Bubble Pressure

If a tube of radius r is immersed vertically in a liquid to a depth h, the local pressure will be $\rho g h$, where ρ is liquid density (more precisely, the difference between liquid density and that of the local vapor environment, but the difference is generally negligible) and g is gravitational acceleration. When air is blown through the tube, it will cause bubbles to form at the immersed end of the tube. Laplace's equation (4.17b) relating the excess pressure on the curved side of the meniscus, Δp, to the principal radii of curvature R_1 and R_2 (both equal to R for a spherical surface) is given by:

$$\Delta p = \gamma_{LV}\left(\frac{1}{R_1} + \frac{1}{R_2}\right) = \frac{2\gamma_{LV}}{R} \tag{4.30}$$

The internal bubble pressure is therefore $\Delta p + \rho g h$. When the bubble first starts to grow, it will have a large value of R, which will then decrease until the bubble becomes a hemisphere. Thereafter, the radius grows again. Thus, when the bubble is a hemisphere, of radius r, the pressure is maximal. Thus maximal bubble pressure,p_{max}, is given by:

$$p_{max} = \frac{2\gamma}{R} + \rho g h \tag{4.31}$$

If the air line is fitted to a pressure gauge, the value of p_{max} may be measured and the value of liquid surface tension,γ_{LV}, then readily calculated (*Fig. 4.7*).

4.4.1.2 Drop Weight

An appealingly simple, but rather inaccurate, method to obtain liquid surface tension values is that of letting a drop accumulate at the end of a circular orifice of radius R, mounted horizontally like a tap. When sufficiently large, the drop will . . . drop. On weighing the fallen

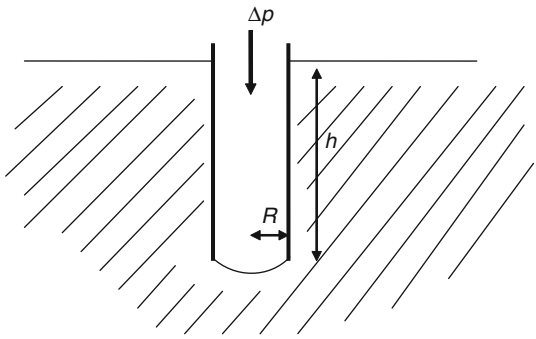

Fig. 4.7
Schematic representation of maximum bubble pressure method

liquid, a pseudo-equilibrium may be drawn between drop weight at separation, mg, and the hitherto surface tension-based retaining force, $2\pi R\gamma_{LV}$. Since some liquid is generally left behind, and since it is not entirely clear that the correct surface tension term to be used is that given above, generally a correction factor, ϕ, is invoked where typically $1 < \phi < 2$. Surface tension is then estimated from:

$$\gamma_{LV} = \frac{mg\phi}{2\pi R} \tag{4.32}$$

There is also a method for estimating γ_{LV} from the shape of a hanging, or pendent, drop *before* it falls, invoking the conflicting effects of gravity and surface tension (Padday 1971, Hartland and Ramakrishnan 1975). However, the mathematical complexities put this beyond the scope of the present text. Briefly, Laplace's equation (4.17b), allowing for *changing* pressure with height within the drop (hydrostatic head), can be rewritten as a second order differential equation. It is this which is solved when drop size is comparable to capillary length (see Chap. 6). The resulting drop profile forms as a "compromise" between gravity (flattening) and surface forces (minimizing surface area, and therefore seeking sphericity) (*Fig. 4.8*).

4.4.1.3 Capillary Rise

A thin, circular capillary tube, of internal radius, R, may be immersed in a liquid vertically and the height of ascension of the liquid within, h, can be used to calculate the surface tension of the liquid, with the proviso that the solid of the tube inner is completely wet by the liquid (i.e., zero contact angle). This is generally assumed for organic liquids, at least, by using glass tubes which have recently undergone some aggressive internal cleaning treatment, such as that by sulfochromic acid or similar. The liquid rises in the tube in order to counteract Laplace's reduced pressure in the meniscus by hydrostatic pressure. For thin tubes, those of interest, having the greatest capillary rise, deviation of the meniscus shape from sphericity may be neglected, and the resulting expression for surface tension is:

$$\gamma_{LV} = \frac{R\rho gh}{2} \tag{4.33}$$

where ρ is liquid density and g, as before, is gravitational acceleration (*Fig. 4.9*)

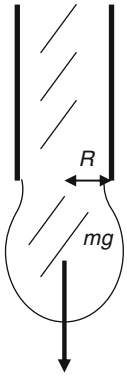

Fig. 4.8
Schematic representation of drop weight method

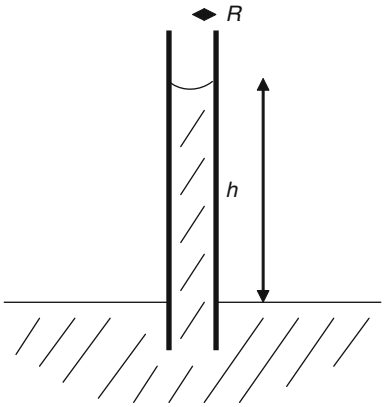

Fig. 4.9
Schematic representation of capillary rise method

4.4.1.4 Wilhelmy Plate

If a smooth, flat solid is immersed in a wetting liquid (i.e., $\theta_0 < 90°$), such that its surface is perpendicular to the horizontal, liquid surface, a meniscus forms toward the upper size, whose effective downward force, or "weight" is given by $\gamma_{LV} \cdot \cos\theta_0$ per unit length measured along the triple line cf. *Fig. 4.10*. Provided a "high surface tension" solid is picked, in general, a platinum plate that has been pre-roughened and pre-cleaned (e.g., by flaming in a Bunsen flame), the contact angle is zero and thus the "weight" per unit length is simply γ_{LV}. If the plate is thin and of length l (along the triple line), the upward meniscus force, F, is $2l\gamma_{\mathrm{LV}}$, neglecting plate thickness. The method described wherein such a platinum blade is attached to a fine balance and meniscus weight evaluated, leading to $\gamma_{\mathrm{LV}} = F/2l$, is known as the Wilhelmy plate technique. It is simple, but complications can however arise. If the plate is too thick, buoyancy must be allowed for, acting on the submerged part of the plate (see *Fibers* below). In some cases, whether the blade is *immersed* or *emersed* from the liquid can give different results, due to wetting hysteresis (see below).

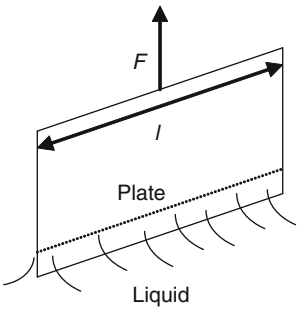

Fig. 4.10
Schematic representation of Wilhelmy plate

4.4.1.5 Du Noüy Ring

This technique (*Fig. 4.11*) is a variation on the Wilhelmy plate, requiring less, expensive, platinum! Notwithstanding, the platinum must be correctly formed into the shape of a circular ring of radius R. The ring is made from circular, platinum wire of sectional radius, ε.

The primary part is thus a torus, although it is attached symmetrically to a small frame allowing it to be attached to a fine balance. The principle is that when the ring is emersed from a liquid, a meniscus will form on both sides of the wire and all around the ring. Neglecting difference in radius for inner and outer circles ($R >> \varepsilon$), it may be expected that the upward meniscus force will be given by: $F = 4\pi R\gamma_{LV}$ (see Wilhelmy Plate). However, spurious effects occur (interference across the ring diameter?) leading to the adoption of an empirical correction factor, β. Liquid surface tension is then given by:

$$\gamma_{LV} = \frac{\beta F}{4\pi R} \tag{4.34}$$

where β is a function of R (and ε). *Table 4.1* gives a few examples of β as a function of R and ε.

4.4.2 Contact Angle

Contact angle is the angle subtended, in the liquid, between the tangent to the liquid/vapor interface and the solid/liquid interface at the triple, or three-phase, line, in the plane perpendicular to this line. In Sect. 4.3, it was shown from thermodynamics that the contact angle at thermodynamic equilibrium, θ_e, is a function of many quantities: the interfacial tensions of the three D-faces, line tension, the curvature of the triple line, and surface profile (cf. 4.28). For real solids in wetting experiments, the list of influences can be extended by surface heterogeneity in terms of locally varying interfacial tension, by adsorption layers, and by other "imperfections." As a result, measured static contact angles *always* show some hysteresis $\Delta\theta$. The so-called static advancing contact angle $\theta_{e,a}$ measured after the triple line has advanced onto a previously unwetted surface area is always larger than the so-called static receding angle, $\theta_{e,r}$, found after the triple line has receded onto a solid surface region that was previously in contact with the liquid

$$\Delta\theta = \theta_{e,a} - \theta_{e,r} > 0 \tag{4.35}$$

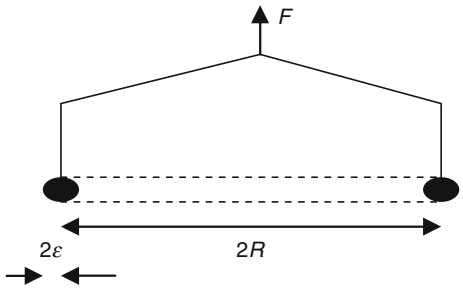

Fig. 4.11
Schematic representation of du Noüy Ring

Table 4.1
Two examples of β for different values of R and ε for the du Noüy ring

R (cm)	ε (cm)	β
1	0.02	0.93
1.85	0.03	0.88

Static contact angle hysteresis summarizes the difference in wetting of real surfaces and of ideally smooth homogeneous solids. The hysteresis can be even larger under dynamic measuring conditions. The static contact angle hysteresis does not depend on the experimental setup used for contact angle measurement provided the same solid and the same liquid are used and equilibrium is attained. As a consequence, the simplified equation (4.29) cannot be applied before the thermodynamic contact angle for the corresponding smooth solid has been deduced from $\theta_{e,a}$ and $\theta_{e,r}$. It should be mentioned that the contact angle hysteresis is not a consequence of (4.28) only. Moreover, gravity causes some kind of stick–slip behavior that depends on the slope of the roughness asperities when the 3-phase boundary moves over the rough solid surface. It can be shown that static contact angle hysteresis depends upon that (e.g., Bartell and Shepard 1953a, b; Johnson and Dettre 1964; Busscher et al. 1984; Bischof et al. 1988).

Various propositions, such as

$$\cos\theta_{\text{meas}} = r \cdot \cos\theta_e \; ; \quad r = \frac{A_{\text{true}}}{A_{\text{geom}}} \text{ (Wenzel 1936)} \tag{4.36}$$

A_{geom} = macroscopic area of the solid surface, i.e., width by length, A_{true} = microscopic area due to surface roughness within A_{geom}.

$$\theta_e = \theta_{e,a} \text{ (Thiessen and Schoon 1940)} \tag{4.37}$$

$$\theta_e = \frac{1}{2}(\theta_{e,a} + \theta_{e,r}) \text{ (Adam and Elliott 1962)} \tag{4.38}$$

have been proposed in the literature to tackle this problem. However, a look at experimental data reveals that none of these formulae solve the problem totally and satisfactorily – cf. *Fig. 4.12* as an example.

Instead, it is clear from experimental results that the functions $\theta_{e,a}(\Delta\theta)$ and $\theta_{e,r}(\Delta\theta)$ follow straight lines

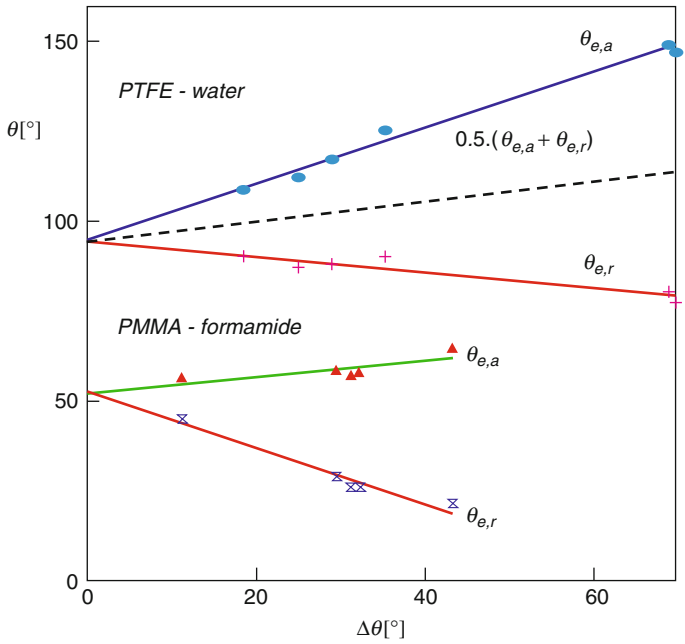

Fig. 4.12

$\theta_{e,a}$ and $\theta_{e,r}$ data measured with various liquids on homogeneous polymer surfaces after stepwise increases of roughness following grinding with abrasive cloth of increasing grade

$$\theta_{e,a} = \theta_e + a \cdot \Delta\theta \tag{4.39}$$

$$\theta_{e,r} = \theta_e - b \cdot \Delta\theta \tag{4.40}$$

As roughness is the cause for $\Delta\theta$ on homogeneous solids, the intersection of these lines with the ordinate is the value θ_e is being sought (Schulze et al. 1989). Hence, the equilibrium contact angle can in principle be determined from a suitable experiment.

In the following sections on experimental methods for contact angle measurement, we shall summarize $\theta_{e,a}$ and $\theta_{e,r}$ as θ_0 will be summarized, for brevity. Of course, advancing and receding angles must be measured for a complete appraisal.

4.4.2.1 Goniometry

Contact angles may be assessed by various techniques, of which a few of the better ones will be mentioned. The simplest involves a plane optical projection of the three interfaces and the triple line. The tangent to the projection of the liquid/vapor interface at the triple line is estimated and the angles measured relative to the flat projection of the possibly rough solid surface. There is equipment on the market to do this, using in the simpler cases an eyepiece with two, independent goniometers, one to align with the projection of the solid surface and one to form the tangent to the projection of the liquid/vapor interface. It is relatively easy to set

up an optical bench arrangement, either to observe the drop directly, or to project its magnified image onto a screen, and then to draw the requisite tangents.

It is, however, always somewhat subjective when placing a tangent to a curve. An alternative method is to use the following procedure. Firstly, when posing a drop on the flat, horizontal surface, ensure from the top that its contact area is circular. (This may be done with a transparent slide, onto which are printed circles of various diameters. By adjustment of drop-to-transparent distance, it is possible to find a position at which a circle should coincide with drop circumference.) Any deviation of the triple line from a circle is a clear proof that the solid surface is either rough or inhomogeneous. You will need the surface tension, γ_{LV}, of the liquid [anyway, to exploit (4.29)], and also its density, ρ. Large drops tend to flatten ("puddles") whereas small drops stay as spherical caps ("dew drops"). The approximate contact radius, $r \approx a$, below which the drop is sufficiently close to sphericity, is given by the liquid's capillary length: $a = (\gamma_{LV}/\rho g)^{1/2}$where g is gravitational acceleration. For water, for example, a is ca. 2.8 mm. Having checked circularity of the contact area and droplet size, θ_0 can be readily estimated from the simple formula for a spherical cap:

$$\tan\left(\frac{\theta_0}{2}\right) = \frac{h}{r} \tag{4.41}$$

where height, h, and radius are as shown in *Fig. 4.1*.

4.4.2.2 "Puddle"

At the other extreme from "dew drops," a "puddle" may form (see *Fig. 4.13*). If the drop radius, r, considerably exceeds a, gravity flattens the liquid bulk. If γ_{LV} is known, e.g., by one of the above methods, then the contact angle may be calculated from a measurement of drop height (in the flat part):

$$\cos\,\theta_0 = 1 - \frac{\rho\, g\, h^2}{2\,\gamma_{LV}} \tag{4.42}$$

As for the pendent drop (above), there exists an intermediate size range between the "dew drop" and the "puddle" for which γ_{LV} may be estimated from drop shape (slightly deformed from sphericity), but its treatment is beyond the scope of this chapter (Padday 1971; Hartland and Ramakrishnan 1975). Modern equipment on the market comes with software that approximates the projection of the liquid meniscus to a solution of the corresponding differential equations.

4.4.2.3 Capillary Rise and Wilhelmy Plate

The principle here is the same as discussed above, the only differences being that the liquid surface tension is assumed to be known and that the contact angle is nonzero. If the θ_0 are

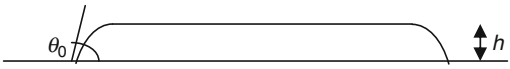

Fig. 4.13
Schematic representation of "puddle" of height h and contact angle θ_0

greater than zero, capillary rise in a tube is less marked, and may even become capillary *descent*, if $\theta_0 > \pi/2$. The liquid level in the tube is lower than the surrounding liquid bath. When the θ_0 are nonzero, (33) includes a term in $\cos\theta_0$ and, after rearrangement, the following expression is obtained:

$$\theta_0 = \cos^{-1} \frac{R\,\rho\,g\,h}{2\,\gamma_{LV}} \tag{4.43}$$

In much the same way, the Wilhelmy plate technique may be used, where force, F, becomes $2\,l\,\gamma_{LV}\,\cos\theta_0$. The disadvantage for both of these is that the solid of interest must be made into a suitable geometric form, which is not always convenient, or even possible!

4.4.2.4 Fibers

The special case of fibers will be given, since knowledge of their surface properties is essential in composite technology. In principle, the method for obtaining contact angle on a fiber is the same as for the Wilhelmy plate: A liquid meniscus forms round the fiber immersed in a liquid bath, and its weight, detected by a microbalance, can be used to obtain θ_0. It is assumed, for simplicity, that the fiber is of circular section of radius r. With F_0 being the force on the balance corresponding to the weight of the fiber before immersion, and F that measured with the fiber partially immersed, vertically, axis perpendicular to free liquid surface and to depth, l, an expression for the difference, ΔF, is obtained given by:

$$\Delta F = F - F_0 = 2\,\pi\,r\,\gamma_{LV}\,\cos\theta_0 - \pi\,r^2\,l\,\rho_L\,g \tag{4.44}$$

In this equation, ρ_L is liquid density (or more precisely, the difference between density of liquid and air) and thus the right hand term is a buoyancy correction. Since the surface tension term scales with r, and the buoyancy term with r^2, clearly the correction becomes very small for thin fibers. (The same basic argument is used when employing a thin Wilhelmy plate, above.)

4.5 Free Energy Balance of Wetting

With the thermodynamic background (cf. Sects. 4.2 and 4.3) and with the experimental steps for getting $\theta_{e,a}$, $\theta_{e,r}$ and the thermodynamic contact angle for the smooth homogeneous solid, θ_e, (Sect. 4.4) the picture can now be completed by discussing the excess Helmholtz free energy of wetting which is often called the Helmholtz free energy of adhesion. Wetting is indeed the adhesion of a liquid on a solid.

Figure 4.14 illustrates the situation before and after wetting at thermodynamic equilibrium. For simplicity, consider a solid with at least one smooth and flat part of its surface. In the initial state (superscript 1), the solid has a phase boundary with the common vapor only. Hence, there are two D-faces with the areas A^1_{SV}, A^1_{LV} in the initial state. Then, the solid is lowered until the flat part of its surface is just isothermally wetted at constant pressure by the flat liquid meniscus. This is the final state (superscript 2) with three D-faces (areas A^2_{SV}, A^2_{LV}, A^2_{SL}) and one triple line. (Any immersion of the solid into the liquid would simply create new area of the D-faces. Such motion only complicates the thermodynamic free energy balance without giving any additional insight.)

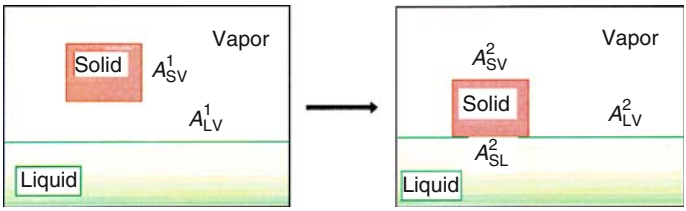

Fig. 4.14

Schematic representation of a solid in vapor (*left*) being led to contact a liquid surface (*right*). A^1_{IJ}, A^2_{IJ} denote the areas of the corresponding D-faces

Note that the constitution of the system, i.e., the components, their number N, their concentrations, and chemical potentials μ_i, as well as pressure and temperature are the same in the initial and the final state. Hence, the state of the bulk phases does not change. Moreover, the interfacial tensions γ_{SV}, γ_{LV} and the 2 N values for the absolute adsorptions $\Gamma_{i,SV}$, $\Gamma_{i,LV}$ will not change either.

Now (4.26) is employed and the excess Helmholtz free energies of all five D-faces may be written

$$F^1_{SV} = \gamma^1_{SV}\, A^1_{SV} + \sum_i^N \mu_i\, \Gamma_{i,SV}\, A^1_{SV} \tag{4.45a}$$

$$F^1_{LV} = \gamma_{LV}\, A^1_{LV} + \sum_i^N \mu_i\, \Gamma_{i,LV}\, A^1_{LV} \tag{4.45b}$$

$$F^2_{SV} = \gamma_{SV}\, A^2_{SV} + \sum_i^N \mu_i\, \Gamma_{i,SV}\, A^2_{SV} \tag{4.45c}$$

$$F^2_{LV} = \gamma_{LV}\, A^2_{LV} + \sum_i^N \mu_i\, \Gamma_{i,LV}\, A^2_{LV} \tag{4.45d}$$

$$F^2_{SL} = \gamma_{SL}\, A_{SL} + \sum_i^N \mu_i\, \Gamma_{i,SL}\, A_{SL} \tag{4.45e}$$

where $\Gamma_{i,IJ}$ = absolute adsorption of component i on the D-face IJ.

A relationship between the areas of the D-faces exists

$$A_{SL} = A^1_{LV} - A^2_{LV} = A^1_{SV} - A^2_{SV} \tag{4.46}$$

Therefore, wetting is considered to be an isothermal, isochoric, and isobaric change of state and the contribution from the triple line is neglected. As a result, the change of Helmholtz free energy of the whole system is given by the change of the excess Helmholtz free energy at the D-faces

$$F^2 - F^1 = F^2_{SV} - F^1_{SV} + F^2_{LV} - F^1_{LV} + F^2_{SL} \equiv F^{wett} \tag{4.47}$$

That is the *excess Helmholtz free energy of wetting*. Inserting (Eqs. 4.45, 4.46), the following equation is obtained

$$F^{\text{wett}} = -(\gamma_{\text{SV}} + \gamma_{\text{LV}} - \gamma_{\text{SL}})\, A_{\text{SL}} - A_{\text{SL}} \cdot \sum_{i}^{N} \mu_i \cdot \left(\Gamma_{i,\text{SV}} + \Gamma_{i,\text{LV}} - \Gamma_{i,\text{SL}}\right) \tag{4.48}$$

and for the specific value (per unit area)

$$f^{\text{wett}} = \frac{F^{\text{wett}}}{A_{\text{SL}}} = -(\gamma_{\text{SV}} + \gamma_{\text{LV}} - \gamma_{\text{SL}}) - \sum_{i}^{N} \mu_i \cdot \left(\Gamma_{i,\text{SV}} + \Gamma_{i,\text{LV}} - \Gamma_{i,\text{SL}}\right) \tag{4.49}$$

which is usually briefly called the *adhesion energy* for the liquid–solid contact.

The first term on the right hand side corresponds to the so-called reversible specific or thermodynamic, work of adhesion (to within a sign change)

$$W^{\text{adh}} = \gamma_{\text{LV}} - \gamma_{\text{SL}} \text{ Dupre's rule} \tag{4.50}$$

as introduced by Dupré (1869). Note that Dupré formulated his rule on an empirical basis long before Gibbs developed the thermodynamics for interfaces in the form used here.

However, there is a second term that covers the energetic contribution from the composition of the three phase boundaries (via the absolute adsorptions) and hence the specific Helmholtz free energy of wetting may not be reduced to a balance of the interfacial tensions involved.

A simple experimental test can be used to demonstrate that this is more than just a theoretical statement. *Figure 4.15* depicts the change of the wetting equilibrium of polymer samples at a Wilhelmy balance (cf. *Fig. 4.10*) owing to a slight compositional change of the common vapor phase. The sample plate at the fine balance consists of either polymer A or polymer B, the test liquid is water, and there is the common gas phase in the compartment (*Fig. 4.15*, left scheme). At the starting point $t = 0$ min (*Fig. 4.15*, plot on the right), the plate just touches the water surface for wetting. The capillary in the setup is still empty so that the common gas phase consists of air and water vapor only. For that equilibrium, the wetting causes a certain force change $F_{\text{meas}}(t = 0)$ as compared to the dry polymer sample A or B. As the next step ($t > 0$), only the vapor phase is contaminated by a small amount of n-octane evaporating from a pendent drop hanging from the glass capillary now (cf. *Fig. 4.15*, left). n-octane is "immiscible" with water. (Note: According to thermodynamics, all substances mix, at least to some extent. Hence, the word "immiscible" corresponds to common usage.) As a saturated hydrocarbon, n-octane forms only weak physical interactions with water and the polymers. Nevertheless, the wetting force $F_{\text{meas}}(t)$ at the Wilhelmy balance changes immediately and significantly whenever a small amount of n-octane vapor is added and then removed! This is due to a change of the wetting equilibrium which in turn is determined by the three D-faces LV, SV, and SL. In fact, this is the type of experiment that may be used to introduce the convenient "spreading pressure," representing reduction in surface tension due to adsorption and mentioned earlier.

For wetting, the extra force acting on the Wilhelmy balance is

$$F - F_0 = L \cdot (\gamma_{\text{SV}} - \gamma_{\text{SL}}) - \text{buoyancy of the sample} \tag{4.51}$$

F_0 = force due to the weight of the dry polymer sample before wetting, L = length of the TL on the wetted polymer sample.

The sample immersion depth does not change when n-octane is added to the composition of the vapor phase and hence the measured change of force is

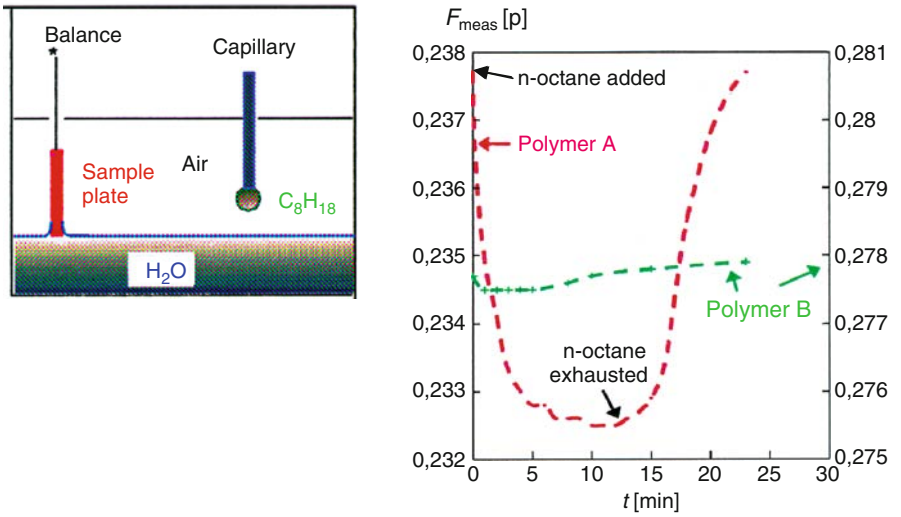

Fig. 4.15

Sketch (*left*) for the Wilhelmy balance with sample plate and a capillary for n-octane evaporation into the common gas phase (air) above the wetting liquid (water). F_{meas} = load change in gram force *p* as measured at the balance. For two polymers A and B (different types of cellulose), the right hand graph shows the quick response of the wetting equilibrium when a little amount of octane is evaporated into the gas phase at t > 0 min and when the atmosphere is replaced by fresh air after some time (return of F_{meas} to the initial value)

$$\Delta F = L \cdot (\Delta\gamma_{SV} - \Delta\gamma_{SL}) = L \cdot [\Delta\gamma_{LV} \cdot \cos\theta_0 + \gamma_{LV} \cdot \Delta(\cos\theta_0)] \tag{4.52}$$

Since $\Delta\gamma_{SL} > 0$, according to (4.26), the change of the wetting equilibrium is accompanied by a change of the specific excess Helmholtz free energy of each D-face:

$$\Delta f_{IJ}^{D} = \Delta\gamma_{IJ}^{D} + \sum_i \left(\Delta\mu_i \cdot \Gamma_{i,IJ}^{D} + \mu_i \cdot \Delta\Gamma_{i,IJ}^{D}\right) \tag{4.53}$$

Therefore, the addition of n-octane to the vapor phase not only changes the interfacial tensions *but* also the chemical potential (via the compositional change) *and* the absolute adsorptions (mainly for the LV and SV interfaces).

As the consequence, an error results from utilizing Dupré's rule (4.50) instead of the full expression (4.49) for the specific Helmholtz free energy of wetting. The magnitude of the error cannot be deduced from wetting experiments since they do not provide information on adsorption at the D-faces in the system.

4.6 Concluding Remarks

It may be seen from the preceding sections that a variety of methods are available to obtain both liquid surface tensions and static contact angles. Some are cheap, or easily constructed, others less so. They all have their various merits, depending on the (geometric) presentation of the solid to be characterized. They also have their respective disadvantages, e.g., the sessile drop

technique is simple, but care must be exercised in assuring correct drop size range and circularity of the triple line; the maximum bubble pressure is precise and capable of measurement of transient surface tensions but generally requires relatively advanced apparatus.

All techniques for contact angle measurement are prone to static wetting hysteresis effects. Wetting hysteresis has its origins in surface roughness, micro-heterogeneities and other "imperfections," and can be of the order of 10 s of degrees. It is rarely less than 2° or 3°, so the commonly seen habit of specifying contact angles to 1, sometimes 2, decimal places is, of course, pointless. This leaves another question: If static advancing and receding contact angles are measured, what is the equilibrium value, θ_e on a flat smooth homogeneous surface? It is θ_e that is needed for Young's equation. The experimental procedure described in the context of (4.39, 4.40) provides the answer.

Bearing in mind the limitations and approximations made for Dupré's rule (4.50) and Young's equation (4.29), finally consider the common treatment of contact angle data which makes use of the combination of the two equations:

$$W^{\text{adh}} = \gamma_{\text{LV}}(1 + \cos\theta_e) \approx -f^{\text{wett}} \tag{4.54}$$

This is the *estimated* specific wetting energy, provided that the surface tension γ_{LV} of the wetting liquid is measured using one of the techniques mentioned and that equilibrium contact angle for the flat surface θ_e is derived correctly from the contact angle hysteresis. Nevertheless, it is unclear whether it is justified to neglect the adsorption terms in the energy balance.

Additional conditions needed for such interpretation of wetting data are as follows:

- Pure liquids that neither swell nor dissolve the solid must be used.
- Solids should be "ideal" (flat, homogeneous, etc.).
- Small curvature of the triple line must be ensured.
- Interfacial tension is an excess property of the phase boundary of *two* phases and responds remarkably to minute changes of the composition!
- The use of literature data for γ_{LV} of liquids should be avoided. Conditions of use can vary.

Finally, there is another price to be paid for using (4.54): The interfacial tensions γ_{SL} and γ_{SV} of the solid have been eliminated, and hence, they cannot be deduced from wetting experiments. This obstacle was the reason for the development of so-called thermodynamic adhesion theories which introduce various proposals for a relationship between the liquid–solid interfacial tension γ_{SL} and the surface tensions γ_{LV}, γ_{SV}. These theories are considered in Chap. 6.

References

Adam NK, Elliott GEP (1962) Contact angles of water against saturated hydrocarbons. Theory of the capillary layer between the homogeneous phases of liquid and vapour II. J Chem Soc doi:0.1039/JR9620002206

Bakker G (1902) Theory of the capillary layer between the homogeneous phases of liquid and vapour II. Zeitschrift für Physikalische Chemie-Stoichiometrie und Verwandtschaftslehre 42:68

Bartell FE, Shepard JW (1953a) Surface roughness as related to hysteresis of contact angles I. The system paraffin-water-air. J Phys Chem 57:211

Bartell FE, Shepard JW (1953b) Surface roughness as related to hysteresis of contact angles II. The system of paraffin-4M-calcium chloride solution-air and paraffin-glyceral-air. J Phys Chem 57:455

Bischof C, Schulze RD, Possart W, Kamusewitz H (1988) The influence of the surface state of polymers on the

determination of the contact angle. In: Allen KW (ed) Adhesion, vol 12. Elsevier Appl Sci, London/New York, pp 1–16

Bumstead HA, Van Name RG (eds) (1961) Scientific papers of J Willard Gibbs, vol 2. Dover, New York

Busscher HJ, van Pelt AWJ, de Boer P, de Jong HP, Arends J (1984) The effect of surface roughening of polymers on measured contact angles of liquids. J Coll Surfaces 9:319

Dupré A (1869) Théorie mécanique de la chaleur. Gauthiers-Villars, Paris, p 369

Gaydos J, Rotenberg Y, Boruvka L, Chen Pu, Neumann AW (1996) The generalized theory of capillarity. In: Neumann AW, Spelt JK (eds) Applied surface thermodynamics. Marcel Dekker, New York, pp 1–51

Hartland S, Ramakrishnan S (1975) Determination of contact angles and interfacial-tension from shape of sessile interfaces. Chimia 29:314

Johnson RE, Dettre RH (1964) Contact angle hysteresis. I. Study of an idealized rough surface. Adv Chem Ser 43:112

Padday JF (1971) The profiles of axially symmetric menisci. Philos T Roy Soc A 269:265–293

Rusanov AI (1978) Phasengleichgewichte und Grenzflächenerscheinungen. Akademie-Verlag, Berlin

Rusanov AI, Prokhorov VA (1996) Interfacial tensiometry, vol. 3. In: Möbius D, Miller R (eds) Studies in interface science, vol 3. Elsevier, Amsterdam/Lausanne/New York/Oxford/Shannon/Tokyo

Schulze RD, Possart W, Kamusewitz H, Bischof C (1989) Young's equilibrium contact angle on rough solid surfaces - I. An Empirical Determination. J Adhes Sci Technol 3:39–48

Shanahan MER, Carré A (1995) Viscoelastic dissipation in wetting and adhesion phenomena. Langmuir 11:1396

Shanahan MER, de Gennes PG (1986) The ridge produced by a liquid near the triple line solid/liquid/fluid. Compt Rend Acad Sci Paris 302:517

Shanahan MER, Cazeneuve C, Carré A, Schultz J (1982) Wetting criteria in 3-phase solid/liquid/liquid systems. J Chim Phys 79:241

Thiessen PA, Schoon E (1940) Besetzung und Adhäsionsarbeit von Oberflächen fester organischer Verbindungen. Zeitschr f Elektrochemie 46:170

Wenzel RN (1936) Resistance of solid surfaces to wetting by water. Ind Eng Chem 28:988–994

Young T (1805) Cohesion of fluids. Philos T Roy Soc A 95:65–87

Zhang J, Sheng X, Jiang L (2009) The dewetting properties of lotus leaves. Langmuir 25:1371–1376